Turbulent Heat Transfer Experiments in Hypersonic Free Flight on Surfaces Representative of Woven TPS Materials

Michael C. Wilder
Aerothermodynamics Branch, NASA Ames Research Center

and

Dinesh K. Prabhu
Analytical Mechanics Associates, Inc.
Aerothermodynamics Branch, NASA Ames Research Center

2021 AIAA SciTech Forum, 11–15 & 19–21 January 2021
Session: TP-18, Aerothermodynamics and Thermal Protection Systems IV
Scheduled: January 20, 2021 from 1:00 PM to 2:15 PM Eastern Time

This work was supported by the Entry Systems Modeling Project of NASA’s Space Technology Mission Directorate

Outline

- Motivation
- Introduction
- Background
- Description of the Experiments
- Results
- Summary and Future Plans

45º Sphere-Cone in Flight at 4 km/s

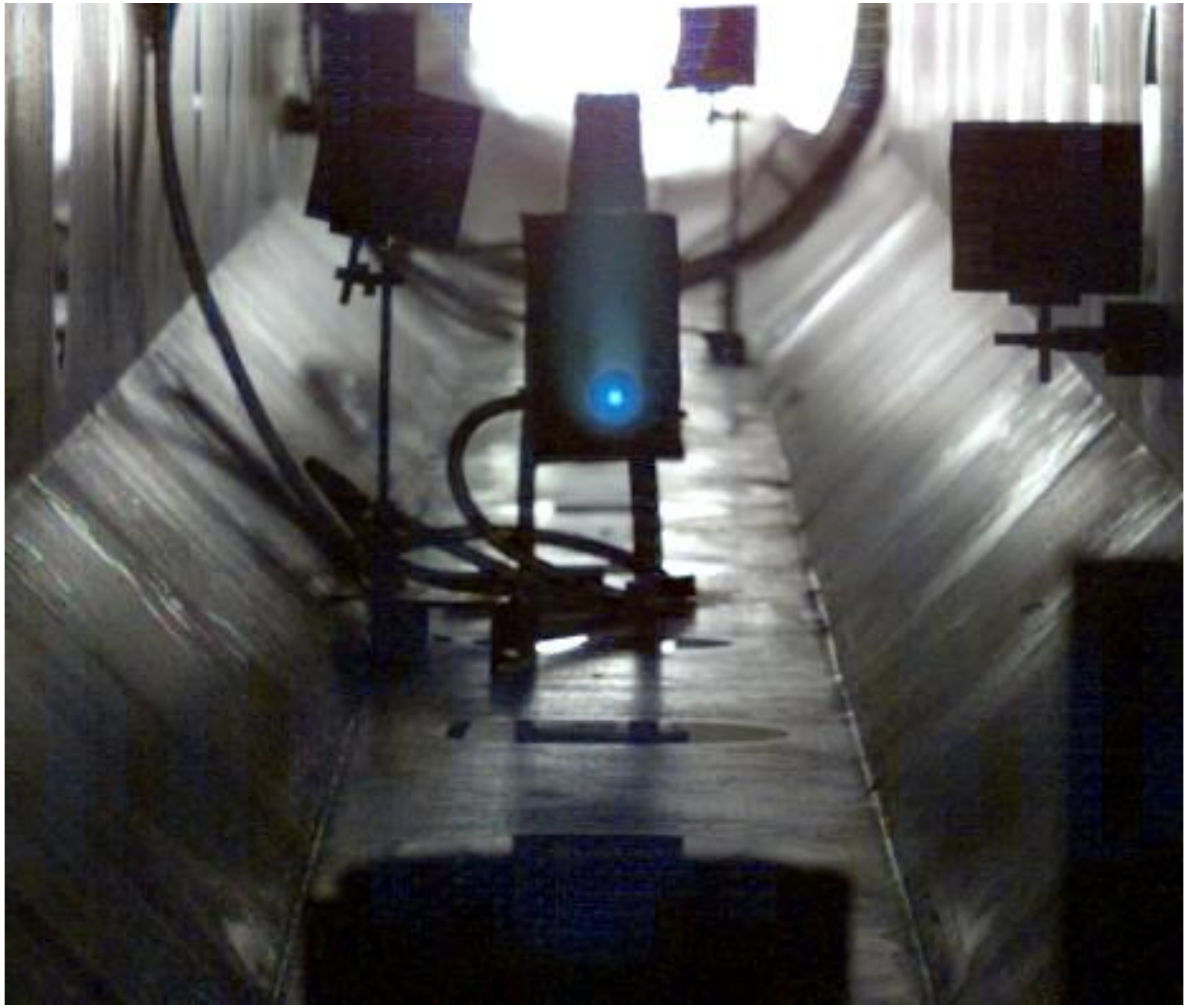

Motivation

- Mars Sample Return Earth Entry Vehicle
  - Baseline forebody TPS is single-layer (insulation layer only) HEEET
  - HEEET is a new class of 3D woven TPS materials developed by the Heatshield for Extreme Entry Environment Technology project
- Test Goal
  - Determine heat transfer augmentation on roughness representative of woven TPS
  - The experimental data will also be useful either in calibrating/validating roughness model(s) within currently used algebraic turbulence models (notably that of Baldwin-Lomax) or in the development of newer models

Dual-Layer HEEET Cross Section

HEEET Surface

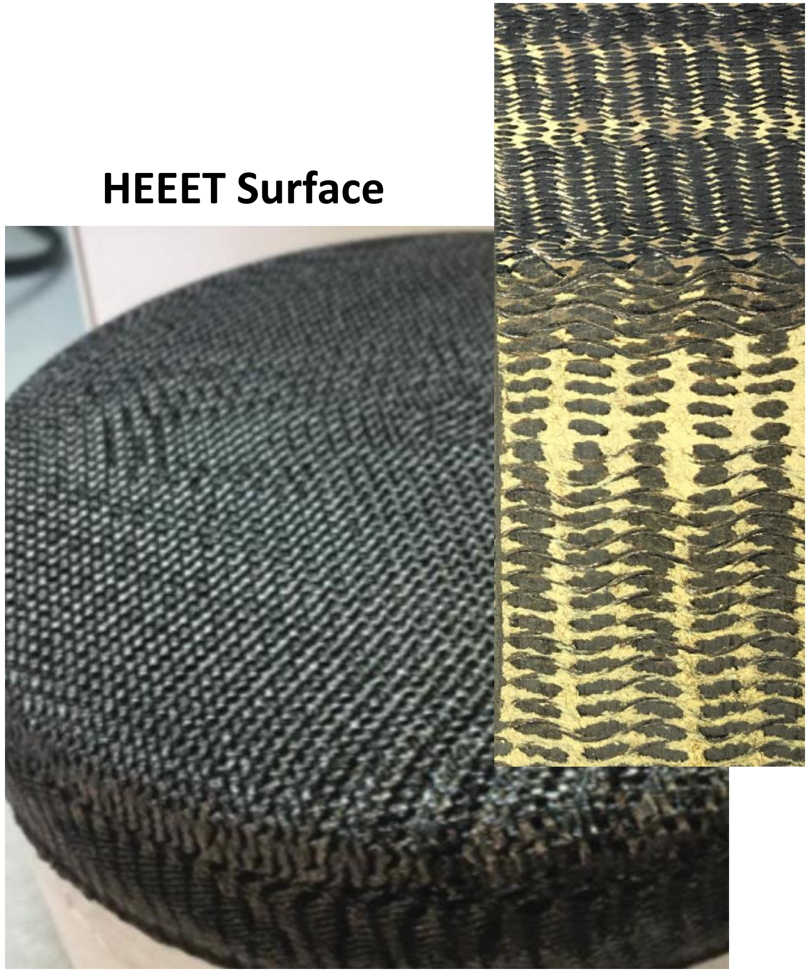

Recession Layer (RL)
- **Densely woven carbon fibers**

Insulation Layer (IL)
- **Looser weave of carbon and phenolic yarns**

Introduction

- Surface roughness can affect the boundary layer state, the heating rates, and skin friction experienced by thermal protection system (TPS) materials
- Real TPS materials have surface roughness characteristic of the material and fabrication, which can evolve during exposure to flight environments (ablation)
- Examples of several types of TPS surface roughness are shown below. This work examines the effects on turbulent heating rates of woven TPS roughness.

Sand-grain

Ablated PICA on Stardust,
Kontinos and Stackpoole
AIAA Paper 2008-1197

Pattern

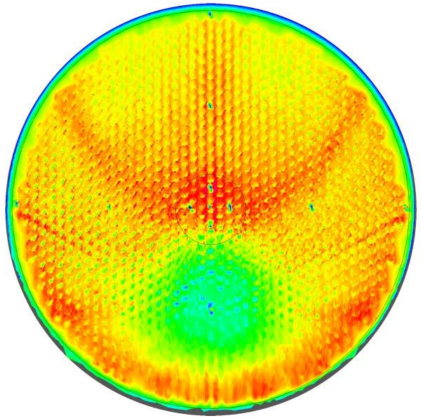

Honeycomb pattern,
Hollis, AIAA 2020-0121

Discrete

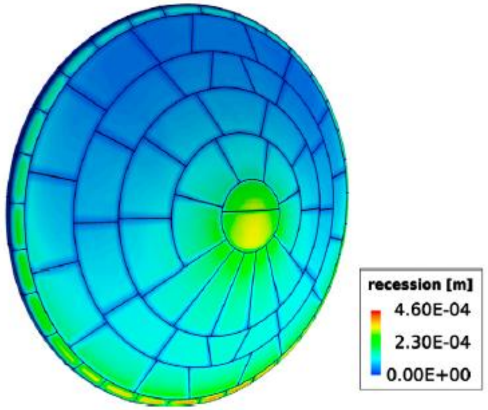

Differential recession on tiled TPS
Meurisse et al., *Aerospace Science and Technology*, 76 (2018)

Woven Pattern

Close-up of the HEEET ETU
https://www.nasa.gov/centers/ames/thermal-protection-materials/tps-materials-development/woven.html

Introduction

- It has been shown that, for sand-grain roughness, heat-flux augmentation correlates with the log of the turbulent roughness Reynolds number, $k^+ = u_{\tau_0} k/\nu_w$, where
  - k is the average roughness element height, and
  - u_{τ_0} $(= \tau_w/\rho_w)^{1/2}$ and ν_w are the friction velocity and kinematic viscosity on a smooth wall

Effect of Sand Roughness on Turbulent Heat Transfer Passive Nosetip Technology (PANT) Program*

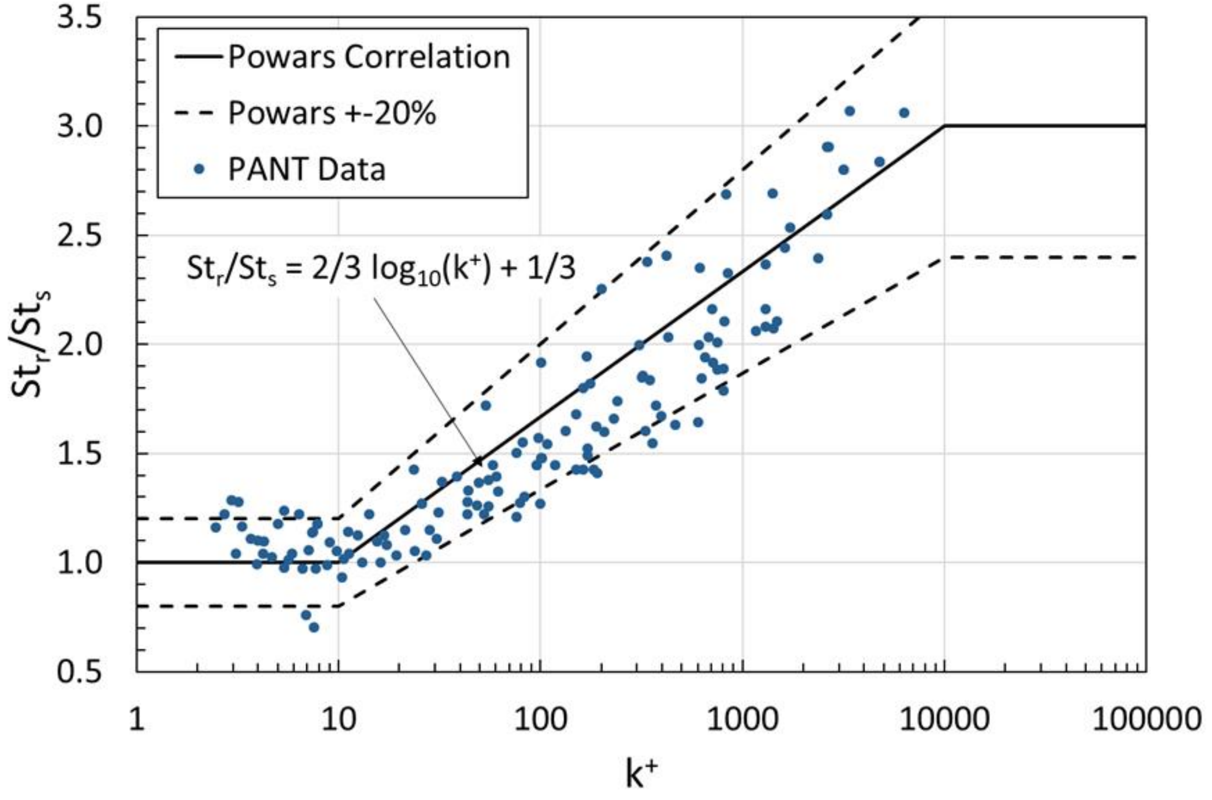

* Wool, M. R., "Final Summary Report Passive Nosetip Technology (PANT) Program," Aerotherm Report 75-159, June 1975.

Introduction

- It has also been shown that heat-flux (and skin friction) augmentation due to pattern roughness depends on the shape and distribution of the roughness elements, as well as the height
  - Many studies, back to (at least) Schlichting[1]
- Various correlations exist to characterize a pattern roughness by an "equivalent sand grain" roughness, k_s, through a shape/distribution parameter, λ (or Λ)

[1]Schlichting, H., "Experimental Investigation of the Problem of Surface Roughness," NACA Technical Memorandum No. 823, April 1937.

Correlation of the Effect of Roughness Density on the Equivalent Sand Roughness[2]

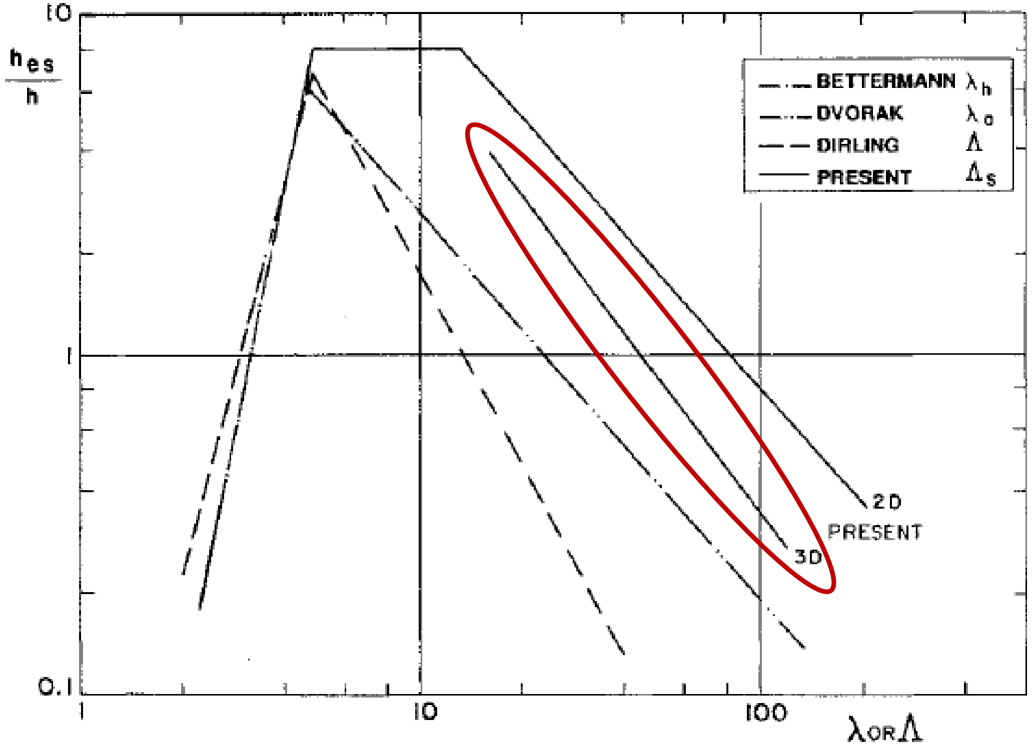

[2]Sigal, A., and Danberg, J. E., ''New Correlation of Roughness Density Effect on the Turbulent Boundary Layer,'' AIAA Journal, Vol. 28, No. 3, 1990.

[3]van Rij, J. A., Belnap, B. J., and Ligrani., P. M., "Analysis and Experiments on Three-Dimensional, Irregular Surface Roughness," Journal of Fluids Engineering, Vol. 124, No. 3, 2002 gives a formulation for the 3D roughness correlation in [2], which is used in this work.

Approach

- Fabricate scale models with surface roughness patterns representative of HEEET weave
  - Model and boundary-layer scales preclude using the actual TPS material (viscous sublayer thickness, δ_s ~ 20 – 30 μm)
  - Patterns, based on scanned HEEET samples were laser etched on metal models
- Fly the models in the hypersonic ballistic range at NASA Ames
  - Tests were done at Mach 9 to 10
  - Roughness Reynolds numbers, k^+ (based on roughness height), between 30 and 300
- Determine convective heat flux from IR thermography
- Compute the smooth-wall boundary-layer parameters required to determine k^+, using the mid-range velocity and measured wall temperature
  - Using the Data Parallel Line Relaxation (DPLR) code

Dual-Layer HEEET Engineering Test Unit

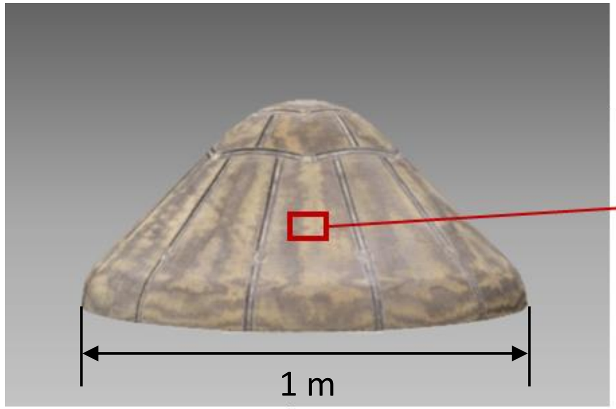

Detail of HEEET Recession Layer

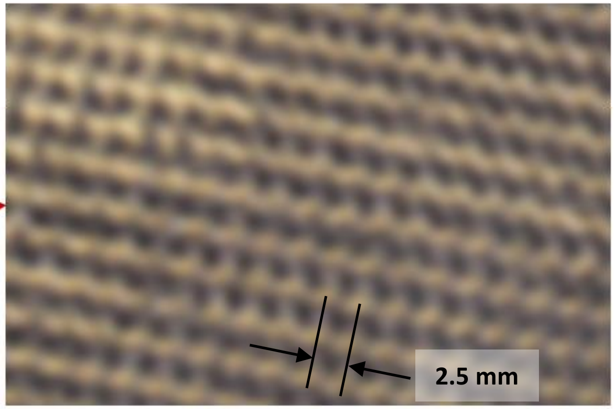

Laser-Etched Ballistic-Range Model

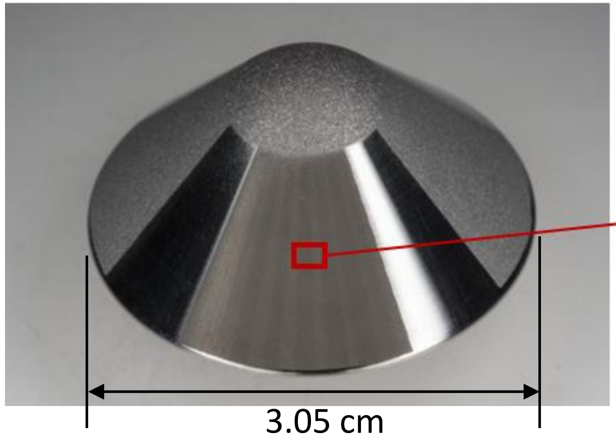

Detail of Ballistic-Range Model Surface

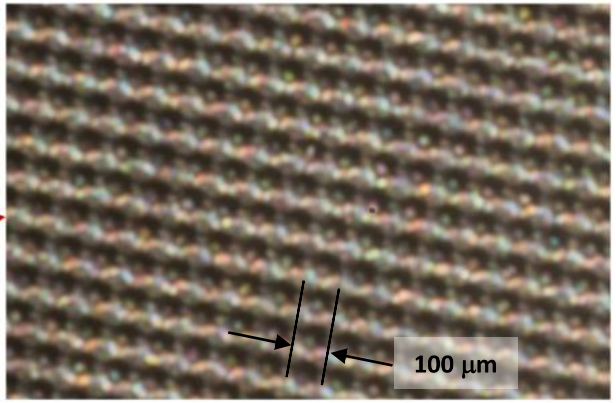

Approach

- HEEET was characterized using 3D surface scans of material samples before and after ablation under turbulent flow conditions

Arcjet-Ablated HEEET Sample*

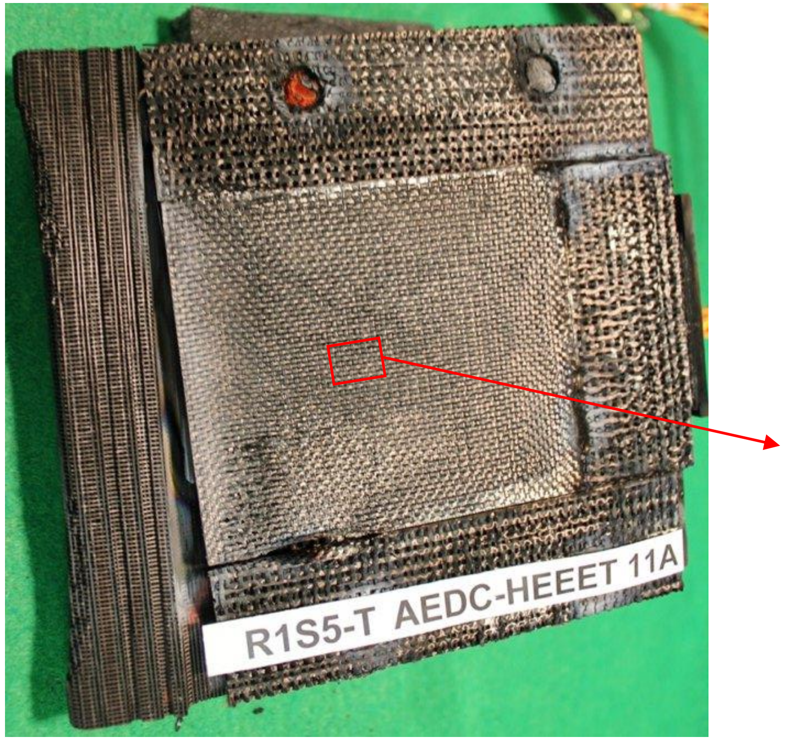

Pre-Test Measurement

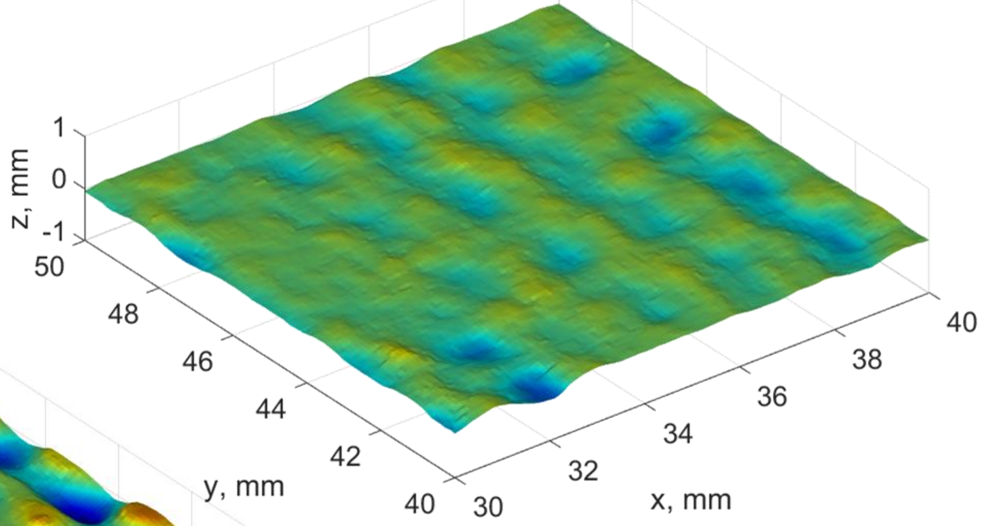

Post-Test Measurement

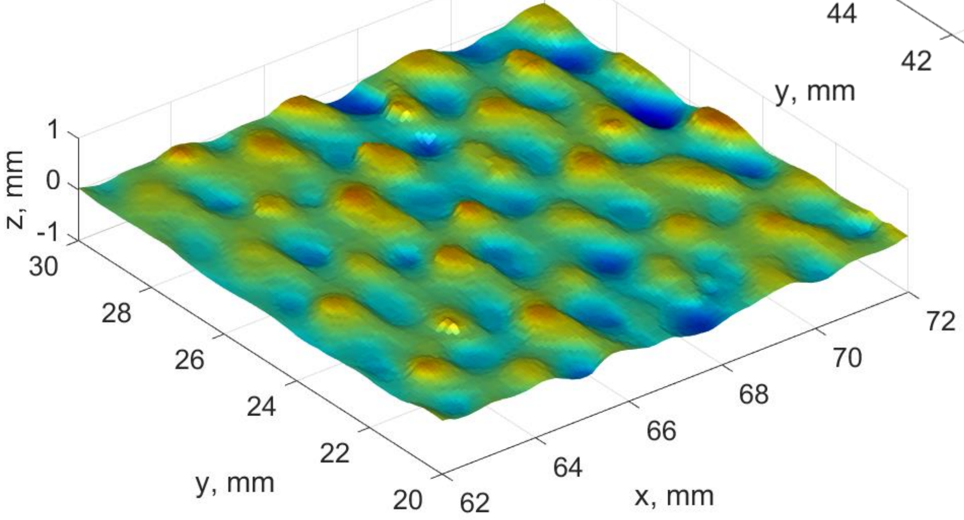

*Venkatapathy, E., *et al.*, "TPS for Outer Planets," Outer Planets Assessment Group (OPAG) Technology Forum; 21-22 Feb. 2018

Approach

- Scaled, idealized, HEEET Recession Layer pattern, and variants, were laser-etched on ballistic-range models:

Ablated HEEET Recession Layer (RL)
(Referred to at RL-20, or 20 μm RL)

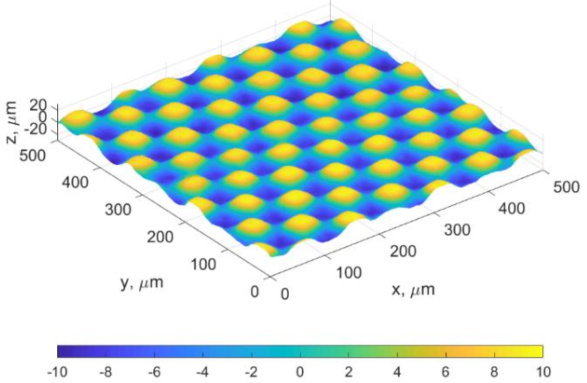

Ablated HEEET RL Distribution with Half the Roughness Element Height
(Referred to at RL-10, or 10 μm RL)

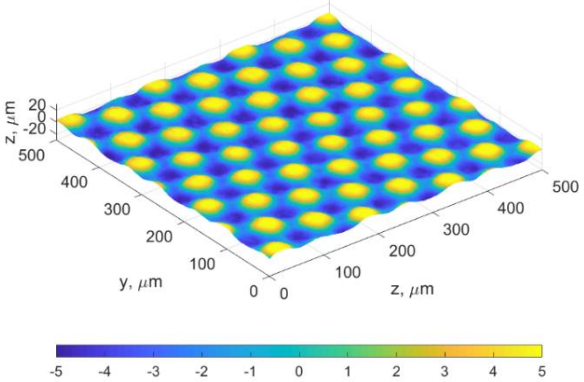

Ablated HEEET RL Distribution with Twice the Roughness Element Height
(Referred to at RL-40, or 40 μm RL)

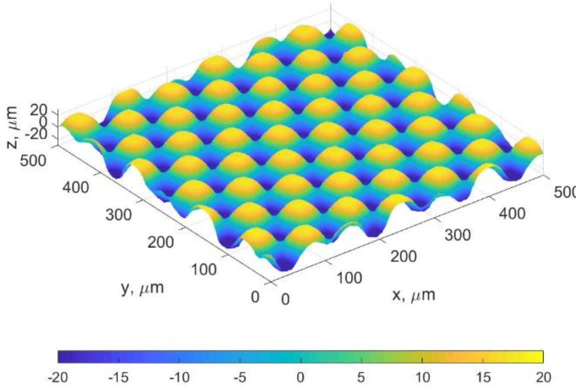

Ablated HEEET Insulation Layer (IL)
Twice the RL Element Height and Spacing
(Referred to as IL)

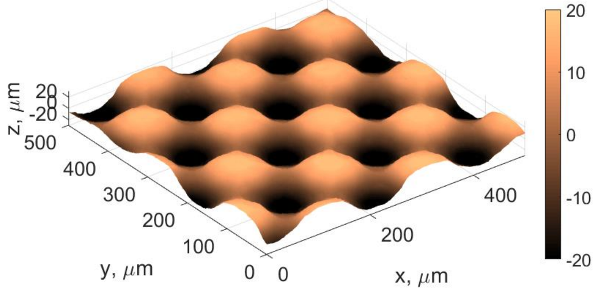

Ablated HEEET IL with Only Element Peaks
(Referred to as PO)

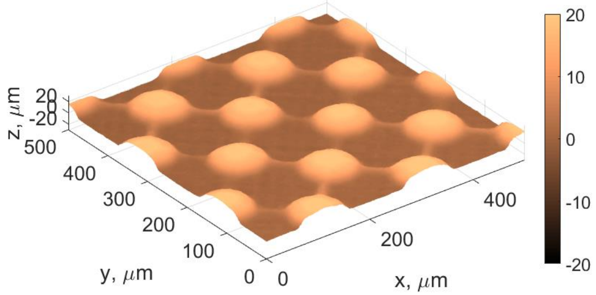

Approach

- Model Geometry and Roughness Layouts:
  - 45^o sphere-cone with R_n = ½ R_{base} (similar to Pioneer-Venus and Galileo probes initial forebody geometry)
  - Base Diameter = 3.05 cm (1.2 in)
  - Each model (each test) had two roughness types, in 60^o circumferential segments, plus smooth-wall segments
    - Either one pattern with two sand roughness sections (grit-blasted), or
    - Two different patterns
  - The nose caps were roughened by grit-blasting to trip the boundary layer for turbulent flow on the cone
  - Models were titanium (Ti-6Al-4V) or stainless steel (type 304)

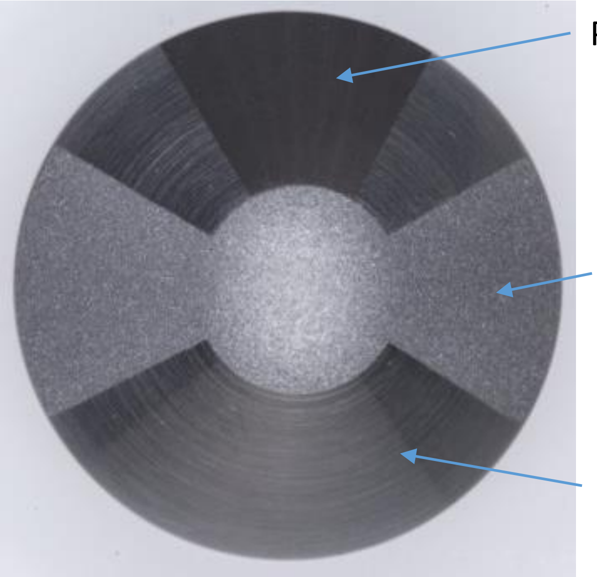

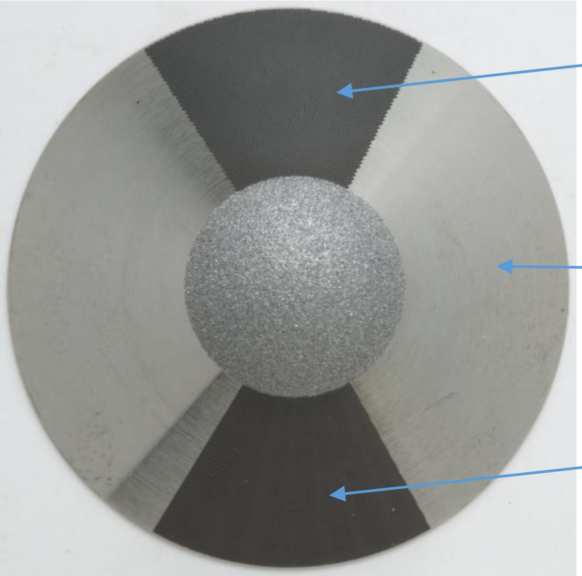

Test Facility

- **Hypervelocity Free Flight Aerodynamic Facility (HFFAF)**
  - NASA's only controlled-atmosphere free-flight aeroballistic range
  - Launch speeds up to ~8 km/s
  - Test section pressure from 1 atm to vacuum
  - Test in various gases (Air, N_2, CO_2, Ar, H_2/He, etc.)
  - Model diameters up to ~30.5 mm (1.2")
  - For additional details, see Wilder, *et al*., AIAA-2015-1339, or visit https://www.nasa.gov/centers/ames/thermophysics-facilities/ballistic-ranges

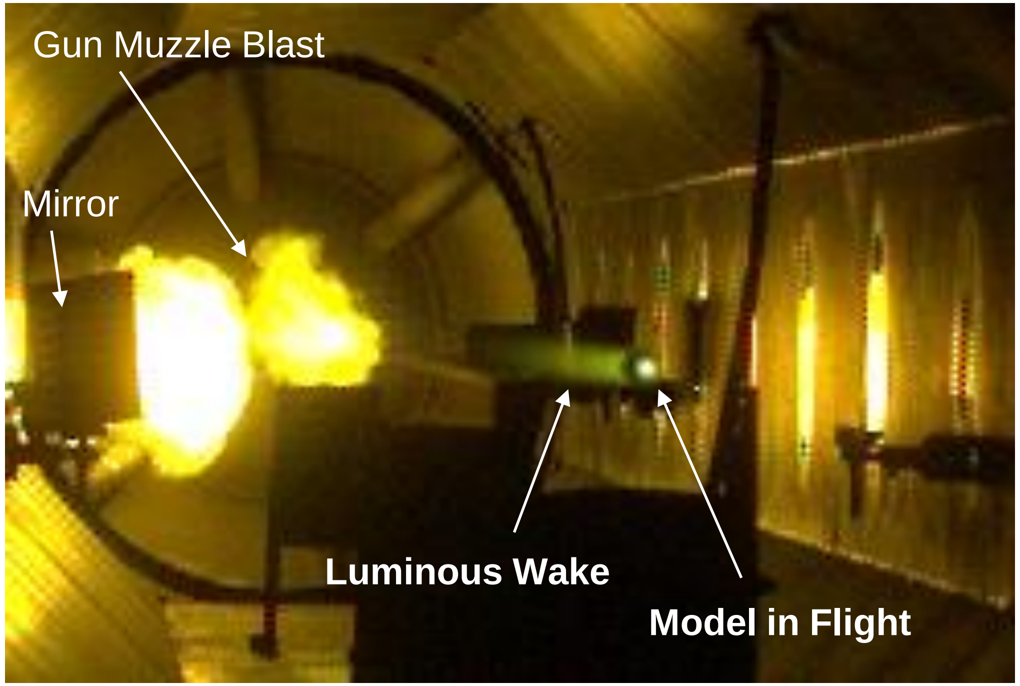

Measurement Approach

- Surface temperature of the projectile is measured using mid-wave IR cameras at three points along the flight path
- The inverse heat conduction problem is solved from the measured surface temperatures given the temperature-dependent thermal properties of the model material
- Details of the measurement approach can be found in Wilder, *et al*., AIAA-2011-3476

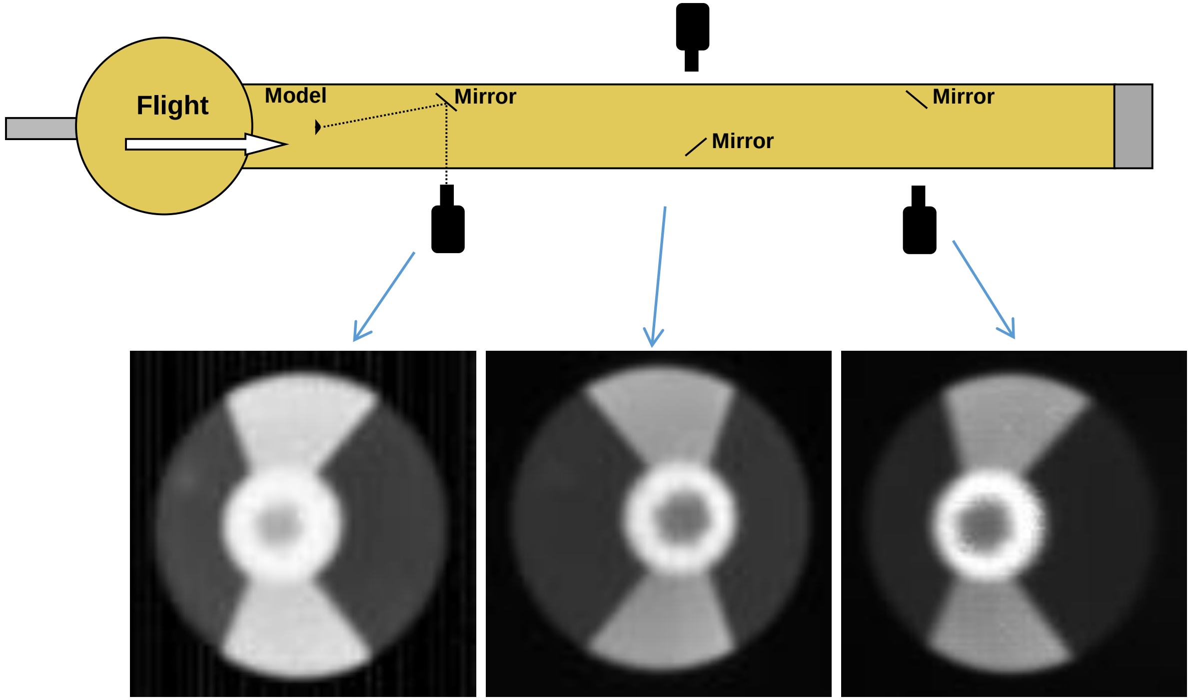

Test Matrix

- Table gives, for each shot, the velocity at launch, and the average conditions (midway through the ballistic range test section)
- Wall temperature and heat flux given are for the smooth-wall sections of each cone at mid-cone, $s/R_n = 1.7$, averaged between $1.55 < s/R_n < 1.85$ and over the circumferential span of each segment
- Results for shots 2805 – 2813 supersede those previously reported in Wilder and Prabhu, AIAA 2019-3009

shot	model	material	V_0, m/s	mid-range V, m/s	Re_D (mid range)	α_{RMS}, deg	T_w, K	$\sigma(T_w)$, K	q_w, W/m^2	$\sigma(q_w)$, W/m^2	Roughness Patterns
2805	MRR 01	Titanium	3257	2994	8.98E+05	2.5	680	3	2.32E+07	2.04E+05	40 μm RL, Sand
2807	MRR 03	Titanium	3322	3058	9.11E+05	2.3	713	8	2.59E+07	6.04E+05	40 μm RL, Sand
2808	MRR 04	Titanium	3221	2967	8.92E+05	14.2	642	5	2.21E+07	3.60E+05	10 μm RL, Sand
2809	MRR 05	Titanium	3215	2957	8.89E+05	2.0	705	3	2.42E+07	2.04E+05	10 μm RL, Sand
2810	MRR 06	Titanium	3247	2984	8.98E+05	2.5	690	4	2.41E+07	2.86E+05	20 μm RL, Sand
2811	MRR 07	Titanium	3210	2951	8.90E+05	2.6	683	5	2.33E+07	3.87E+05	20 μm RL, Sand
2812	MRR 08	Titanium	3117	2870	8.60E+05	4.5	640	3	2.16E+07	2.08E+05	10 μm RL, Sand
2813	MRR 09	Titanium	3112	2861	8.60E+05	2.8	641	3	2.20E+07	2.10E+05	20 μm RL, Sand
2814	MRR 11	Steel	3422	3156	1.58E+06	3.0	666	5	4.21E+07	6.37E+05	20 μm RL, Sand
2832	MRR 16	Titanium	3256	2996	9.10E+05	2.0	675	4	2.29E+07	3.51E+05	IL, PO
2833	MRR 17	Titanium	3230	2975	9.01E+05	3.0	709	4	2.31E+07	2.36E+05	IL, PO
2834	MRR 10	Titanium	3243	2980	9.09E+05	5.7	678	5	2.31E+07	4.00E+05	20 μm RL, IL
2836	MRR 18	Titanium	3248	2831	1.43E+06	2.6	774	4	3.34E+07	3.57E+05	IL, PO
2837	MRR 19	Titanium	3185	2699	1.65E+06	4.4	786	6	3.58E+07	5.85E+05	IL, PO
2840	MRR 20	Titanium	3498	3126	1.25E+06	2.1	812	4	3.65E+07	3.91E+05	IL, PO
2843	MRR 12	Steel	3528	3259	1.60E+06	2.2	618	2	4.53E+07	3.96E+05	10 μm RL, Sand
2844	MRR 15	Steel	3539	3263	1.61E+06	1.4	674	3	4.47E+07	4.56E+05	20 μm RL, IL

Example Heat-Flux Profiles

- For each shot, mean profiles were determined by averaging circumferentially through a given surface texture area
- Mean profiles for a given texture were averaged across multiple shots at the same conditions
- Error bars in the plot represent shot-to-shot standard deviation of the mean profiles,
  - except for the laminar-flow data (only one shot), and the RL-40 data (only two shots), where the error bars represent circumferential standard deviation for one shot

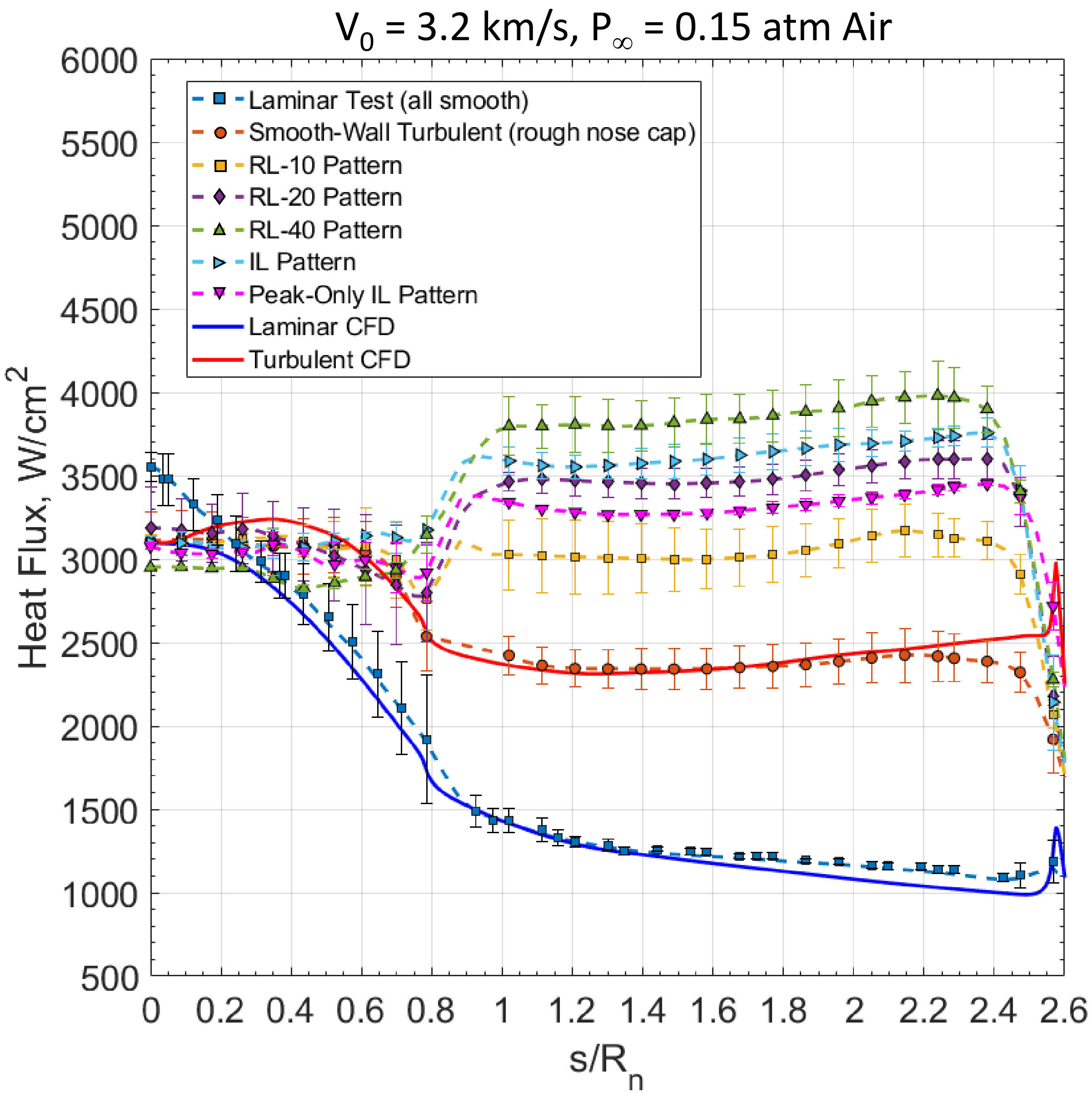

Example Heat-Flux Profiles

- Comparisons between heat flux augmentation, q_r/q_s, on pattern and sand (grit-blasted) roughness
  - As expected, pattern roughness with a given roughness element height, k, appears smoother (lower q_r/q_s) than a sand-roughened surface with the same mean roughness element height
  - Plot compares tests made at the same freestream conditions, and for one pattern distribution (the RL patterns)

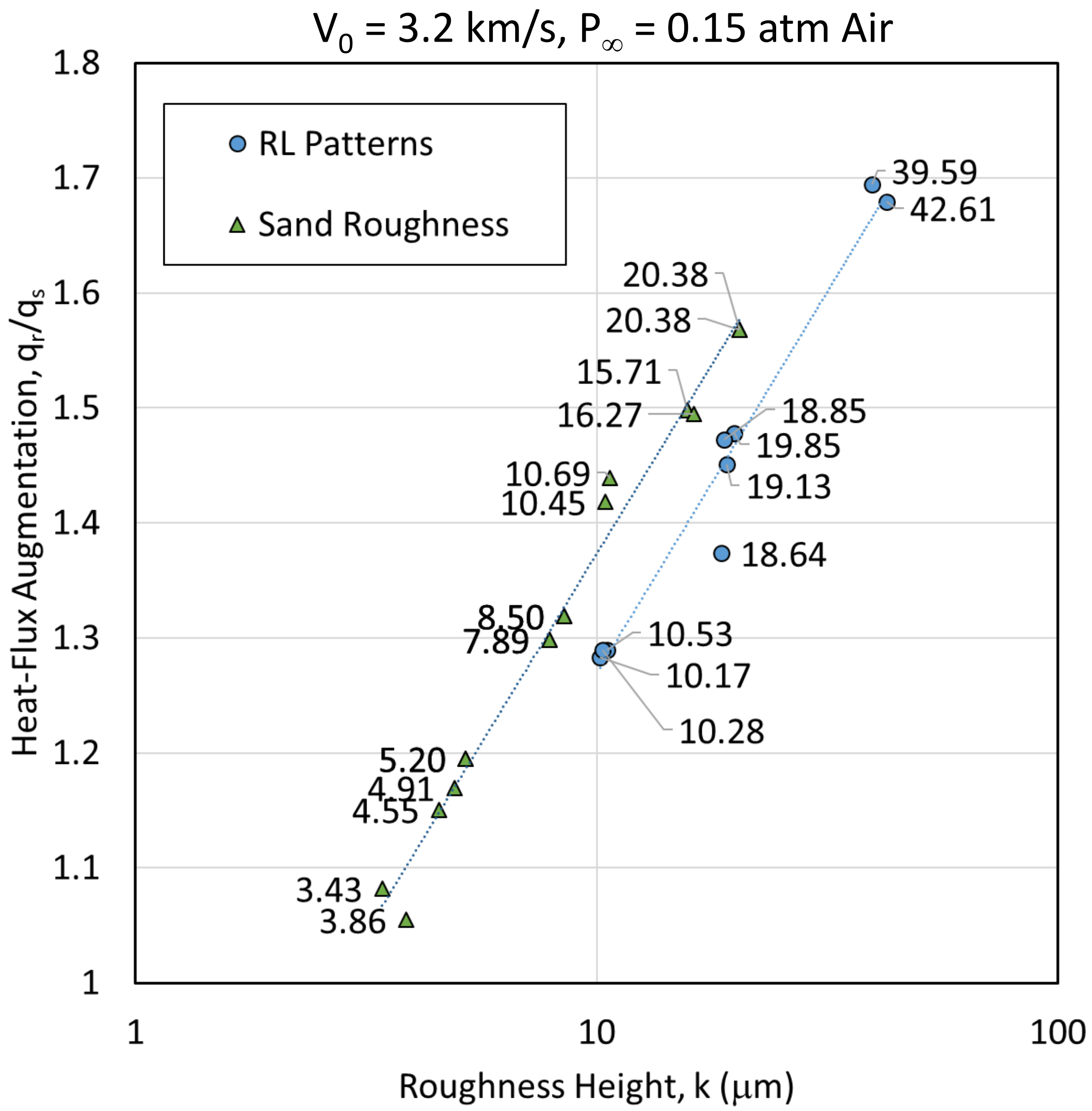

Results

- Results to date
  - Heat-flux augmentation correlates reasonably well with the log(k^+), with k^+ based on the mean roughness element height, k
  - Augmentation for the pattern roughness was less than for sand roughness of the same mean k
  - Observed no strong dependence on the roughness element shape for the patterns tested

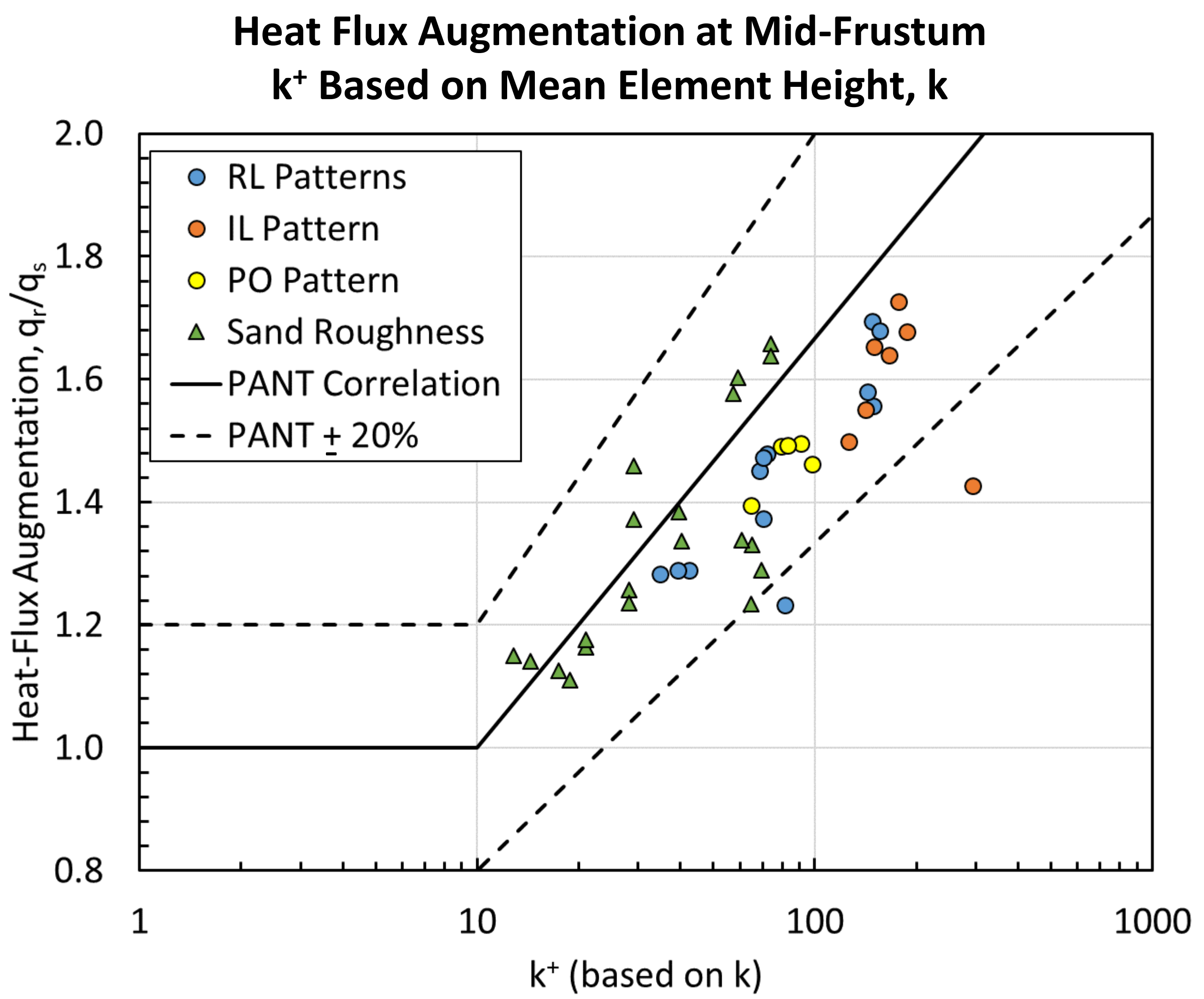

Results

- Results to date
  - Heat-flux augmentation does not correlate as well with k_s^+, especially for the 10 μm Recession Layer (RL) pattern, and the "Peaks-Only" (PO) pattern
    - Equivalent sand grain height determined using the formulation of van Rij, et al. [3], of the 3D roughness correlation of Sigal and Danberg [2]

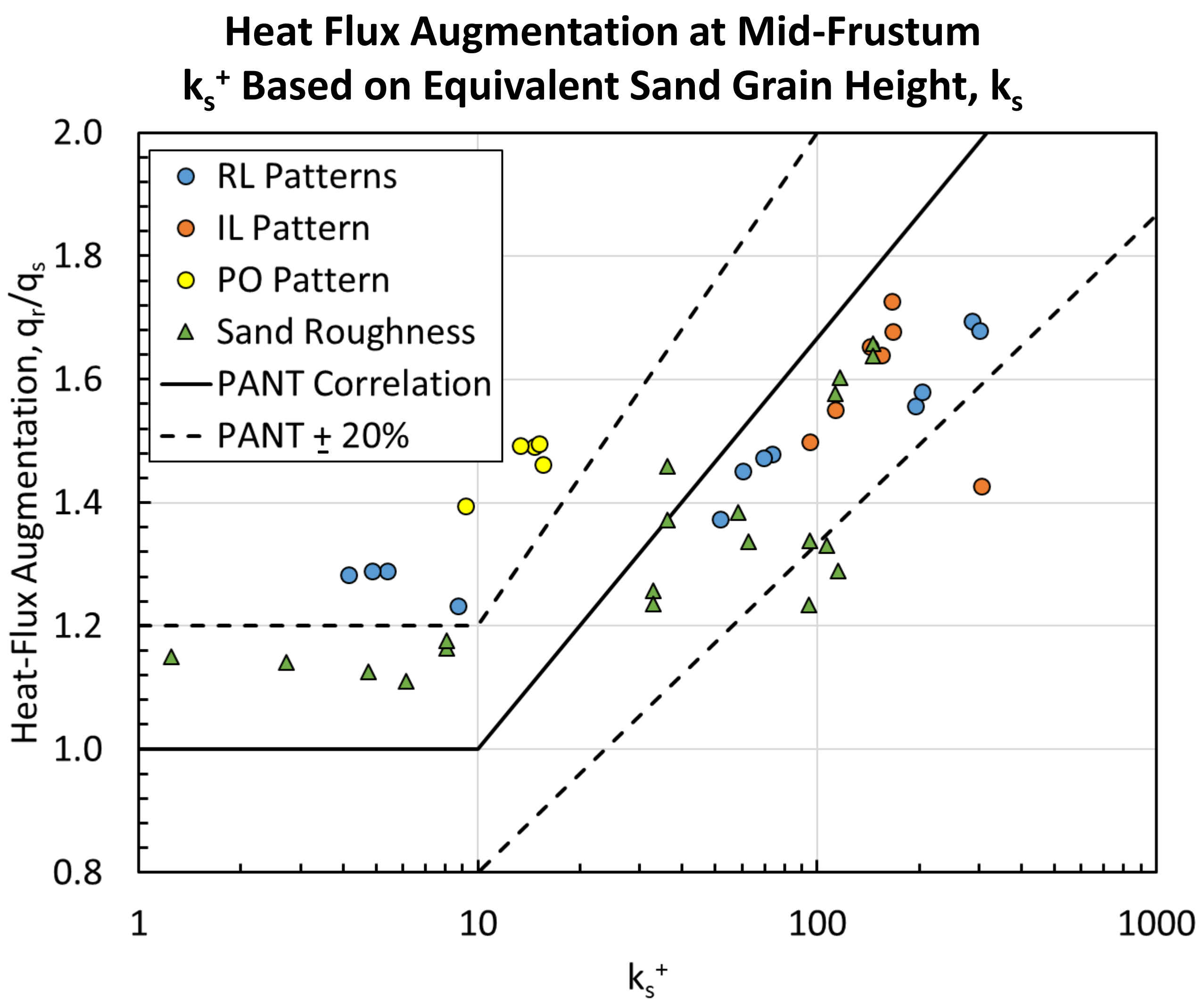

Summary and Future Plans

- Measurements of turbulent rough-wall heat flux have been made in hypersonic flight in a ballistic range to characterized heat-flux augmentation on roughness patterns representative of woven thermal protection system materials
- Reference measurements were also made on sand grain roughness
- Heat-flux augmentation for the roughness patterns was less than for sand roughness of the same mean roughness element height, k
- The heat flux augmentation for both pattern and sand roughness correlated with the roughness Reynolds number, k^+, when the characteristic height was the average height of the roughness elements, k
- The results did not correlate as well with k_s^+ when using existing equivalent sand grain correlations to determine k_s for this pattern roughness
- Additional tests are planned for 2021

National Aeronautics and
Space Administration

Ames Research Center
Entry Systems and Technology Division